VOL. 17, NO. 13, JULY 2022 ISSN 1819-6608
ARPN Journal of Engineering and Applied Sciences

www.arpnjournals.com

SYNTHESIS AND CHARACTERIZATION OF ZrO_2:Al_2O_3 CERAMICS NANOCOMPOSITE

Ahmed A. Thamir[1], Najwa J. Jubier[1] and Jafer F. Odah[2]
[1]Department of Physics, College of Science, Wasit University, Wasit, Iraq
[2]College of Science, Al-Karkh University of Science, Baghdad, Iraq
E-Mail: ahmedkh224@uowasit.edu.iq

ABSTRACT

Ceramic nanocomposites ZrO_2:Al_2O_3CNcwas produced successfully using the sol-gel method. Use zirconium nitrate and aluminum nitrite mix with sodium hydroxide as reaction fuel by ratio 1:3 mol. Different techniques were used to study the physicochemical characterization of ZrO_2:Al_2O_3CNc; XRD to analyze the crystal structure. The crystallinity and morphology of the product were confirmed using X-ray diffraction (XRD), where X-ray diffraction shows that the prepared ZrO_2:Al_2O_3hasa crystalline nature. FESEM and EDX. for morphology, size, and elemental composition. FTIR was used to study the chemical bound and functional group. Perfect binding was obtained of the, (ZrO_2:Al_2O_3) Inter phase boundaries with no discernible delamination or cracks confirmed by (FESEM) observations. Most particles have a uniform distribution in a spherical shape with an average particle size of ~10nm.

Keywords: ZrO_2:Al_2O_3, ceramic nanocomposite (CNc), sol-gel method.

1. INTRODUCTION

The search for bone substitutes is urgent due to the high number of fractures resulting from auto accidents. Millions of dollars are spent worldwide on bone substitutes, affecting the economy-especially in underdeveloped countries [1]. Biocompatibility and mechanical strength are two advantages of these materials. Ceramics materials such as zirconium oxide (ZrO_2) and alumina (Al_2O_3) are utilized globally for bone regeneration, making them appropriate for load-bearing and wear-resistant applications. [2] However, alumina brittleness can cause fractures, and zirconia can age due to hydrothermal deterioration in the presence of water [3]. To prevent the low-temperature deterioration that occurs after long-term implantation in the human body. Many zirconia-alumina composites have recently been produced to reduce ageing and improve mechanical characteristics.[4]from zirconia transformation toughening without the substantial disadvantage of ageing, advanced alumina/zirconia composites are prime candidates for load-bearing components in hip and knee artificial. They also offer increased strength and fracture resistance, resulting in increased implant dependability and longevity. [5] The clinical success of a new ceramic material lies not only in its mechanical properties but also on events that happen mainly at the tissue-material interface and determine its integration into the bone) [6] There is a lot of literature associating the enhancement of the initial attachment of osteoblasts or their precursors onto biomaterial surfaces with better bone-implant integration). [7, 8]On the other hand, the degree of scaffold porosity influences the bioactivity of ceramics. Cell migration, proliferation, and vascularization are all aided by the addition of linked pores. Bone tissue development is enabled by effective fluid circulation and nutrient delivery through the pores, while the increased surface area of porous structures leads to improved bonding with host tissues. The mechanical characteristics of the scaffold are compromised when porosity increases. Porosity, pore size, these factors must be considered to achieve the required mechanical and biological functions. Bimodal-pore ceramics, which feature pores in two different sizes ranges, have been proposed to have excellent mechanical characteristics and have a strong chance of being employed in biomedical applications. Solid and bimodal-pore zirconia/alumina composites may be beneficial in terms of mechanical characteristics and biological behavior in this situation.[9-12]

2. EXPERIMENTAL

2.1 Materials and Method

The materials used in this study were: zirconium nitrate (Zr (NO_3)4), which was procured from Sigma-Aldrich, Germany, and Sodium Hydroxide (Avonchem Ltd) was used as the zirconium precursor. ZrO_2 NPs were prepared from (Zr (NO_3)4) and NaOH with 1: 3 ratios. Also, Aluminum nitrate (Al (NO_3)3.9H_2O) was procured from Riedel-de Haën Sigma-Aldrich Germany; Alumina was prepared using aluminum nitrate and sodium hydroxide in a mixing ratio 1:3 ratios.

2.2 Method of Sample Preparation

ZrO_2 were synthesized by using a sol-gel method at alkaline (pH9). The reaction was performed at 50 °C under vigorous stirring at 700 r.p.m. Firstly, the "sol" was prepared by dissolved (33.924g) from (Zr (NO_3)4) in 100ml of deionized water and stirred at 700 rpm using a magnetic stirrer at 50 °C. To produce a sodium hydroxide solution, one mole (12 g) of sodium hydroxide pellets were dissolved in 300 ml deionized water and stirred at 700 rpm with a magnetic stirrer at 50 °C to produce a sodium hydroxide solution. Add (Zr (NO_3)4) solution drop by drop to sodium hydroxide was added while continuously stirring. The color less solution becomes a white precipitate when sodium hydroxide is added to it. The same procedure was followed to prepared alumina. Upon completing the preparation of the two materials and

at the stage of gel formation, 100 ml of zirconium oxide was mixed with 100 ml of alumina. Continuing the mixing process using the magnetic mixer at a temperature of 50 ℃and for half an hour after the mixing process, the mixture was placed in an Ultrasonic Cleaner bath device at 60 °C for 2hrs.

After the preparation of the gel, the gel was washed several times with distilled water to remove impurities. The gel was also filtered by using filter paper placed in a glass funnel. To obtain the final ZrO_2:Al_2O_3CNc, the drying and calcination process are necessary. Firstly, the drying process involves removing the remaining liquid (solvent) phase. The gel was dried at 70˚C by using a drying oven (Binder FED 53-UL Forced Convection Drying Oven) for 6 hours, typically followed by a significant amount of shrinkage and densification. The resulting powder was milling using a mortar and pestle. Secondly, the calcination process involves forming a Nanocrystalline powder. The specimens were calcined at 800˚C for 1 hour and sintered at 1000℃ for 4 hours using a firing furnace (shin sheng furnace, Korea).

3. CHARACTERIZATIONS

- With a Philips diffractometer produced in Japan, X-ray powder diffraction profiles were acquired using Cu Ka radiation (0.1541 nm) and a continuous scan in the range 5-90°.
- To study the morphology of ZrO_2:$Al_2O_3$was used a Field Emission Scanning Electron Microscope (FEI NOVA NANOSEM 450I) The instrument is endowed with quadrant semiconductor diode detectors for secondary and backscattered electrons collection, respectively, and an Energy Dispersion Spectroscopy analyzer for elemental analysis. All the samples were observed in High Vacuum mode, then a golden layer of about 10 nm was applied on their surface before the investigation to prevent any charging effect. Secondary electrons were used to observe the ZrO_2:Al_2O_3CNc. In contrast, backscattered electrons were collected for obtaining composites images, with the purpose to enhance the difference, then allowing better observation of the distribution of the ZrO_2:Al_2O_3particles. All the materials have been observed using 20 kV of voltage. FESEM analysis was performed studying dispersion and distribution of ZrO_2:Al_2O_3CNc.Energy Dispersive X-Ray Spectroscopy Analysis (EDX) (company (FEI NOVA NANOSEM 450I) were used to examine the composition of element material that constitute the samples, this analysis was also used to identify the chemical composition of the ZrO_2:Al_2O_3CNc.
- FTIR spectroscopy was used to find the presence of the functional group in the ZrO_2:Al_2O_3CNc.

4. RESULTS AND DISCUSSIONS

4.1 X-Ray Diffraction Analysis

The sample's crystalline nature was investigated using X-Ray Diffraction. Figure-1 shows ZrO_2:Al_2O_3(CNc) XRD pattern peaks with polycrystalline phases tetragonal zirconia (T-ZrO_2) and alpha-alumina (α-Al_2O_3). The characteristic peaks of the T-ZrO2 match with C.O.D file no: 96-153-9832. has three sharp peaks (2θ) at (30.32o), (50.06o) and (60.06o) can be well match with Millar indices (111), (202) and (311). α-Al_2O_3 matched with C.O.D file no: 96-152-8428. It has several peaks at 2θ equal to 34.36˚, 50.06, 59.10 and 72.84 can be well match with Millar indices (002), (012), (110) and (201) agree well with earlier studies. [13, 14] From the results obtained, we conclude that zirconia is more crystalline than as-formed alumina as shown in Figure-1 that alumina peaks are less sharp than zirconia peaks. This observed difference may be due to the crystallinity of zirconia. This is because the crystallization of zirconium oxide starts at lower temperatures in those systems containing both substances. The Scherrer formula was used to determine the crystallite size of the particle. [15]The resulting average crystallite size was to be ~12 nm.

4.2 FE-SEM / EDX Analysis

The morphology and particle size of ZrO_2: Al_2O_3(CNc) were investigated by FESEM, as shown in Figure-1 specimens calcined at (1200°C) with different magnification (FESEM). It was observed through the scanning electron microscope images that the samples were prepared by sol-gel using zirconium nitrate and aluminum nitrate with sodium hydroxide as fuel for the reaction in comparison with the researcher's work .[16]The ceramic compounds contained spherical particles, uniform particle distribution, and an average size equalto ~10nm.
A particle size distribution histogram determined from the (FESEM) images showed a variation in the particle size. The particles are in the range of 10–12 nm with an average diameter size of -10 nm (Figure-5).

4.3 FT-IR Spectroscopy Analysis

Figure-5 shown FTIR spectra ZrO_2: Al_2O_3CNcproduced by the sol-gel technique and calcined 4 hours at 1000 °C. have absorption band in the 500-1502 cm-1 owing to the O-Al-O related to α-Al2O3 [17]. The O–H stretching vibration and bending frequency of the ZrO2 molecule also appeared at 1520.27, and 2963.4 cm-1 and Zr-O-Zr vibration exhibit a sharp band in the Zr-O-Zr region, suggesting a substantial influence of the synthesis of ZrO_2:Al_2O_3. The absorption band is around 2963.4 cm-1 to 3563.8 cm-1 stretches and bends to the O-H vibrations bond, which means the presence of a water molecule in the sample [18, 19].

5. CONCLUSIONS

The present study produced ZrO_2:Al_2O_3CNc using the sol-gel method. The XRD results revealed that the stoichiometric amount of alumina-to-zirconia exhibited a crystal structure at 1000 c and was characterized by a very high homogenous ratio and perfect bonding at the ZrO_2:Al_2O_3interphase boundaries. An absence of cracks or delamination. FESEM /EDX result, a uniform distribution of ZrO_2 grains in the Al_2O_3 matrix was observed. FESEM analysis also shows that most particles have a uniform

distribution in a spherical shape with an average particle size of ~10nm.FTIR spectra of ZrO_2:Al_2O_3CNc showed several peaks of the significant functional groups O-H stretch or the N–H, stretching vibrations C=C of ketene, C-H bend of unsubstituted alkane. This confirms the formation of groups of both oxides because of the high homogeneity between the materials prepared by the sol-gel method used to prepare ceramic compounds.

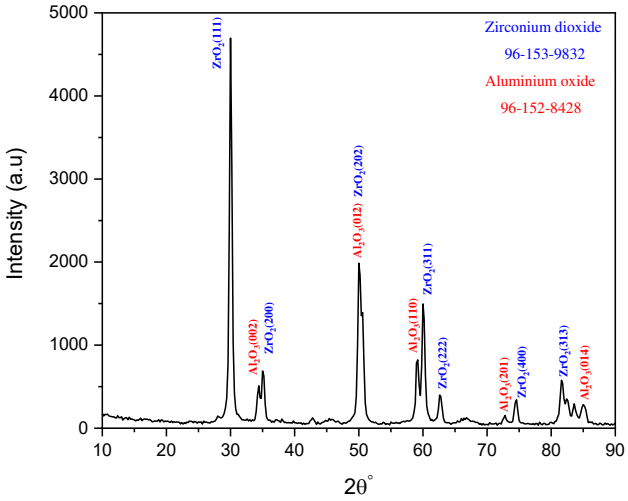

Figure-1. XRD pattern of ZrO_2:Al_2O_3 CNc.

Table-1. Structural parameters of ZrO2:Al2O3 nanostructures obtained from the X-ray diffraction (XRD).

2θ°(Deg.)	Phase	(hkl)	d_{hkl} Exp(A°)	d_{hkl}std(A°)	Crystallite size (nm)
30.32	T-ZrO_2	111	2.9	2.9	13.71787325
50.06	T-ZrO_2	200	1.820	1.800	10.95961873
60.06	T-ZrO_2	202	1.539	1.535	15.29341663
34.36	α-Al_2O_3	002	2.607	2.494	8.315305248
50.06	α-Al_2O_3	012	1.820	1.831	10.76769498
56.1	α-Al_2O_3	110	1.638	1.556	12.00164404
72.84	α-Al_2O_3	201	1.297	1.301	15.34065684

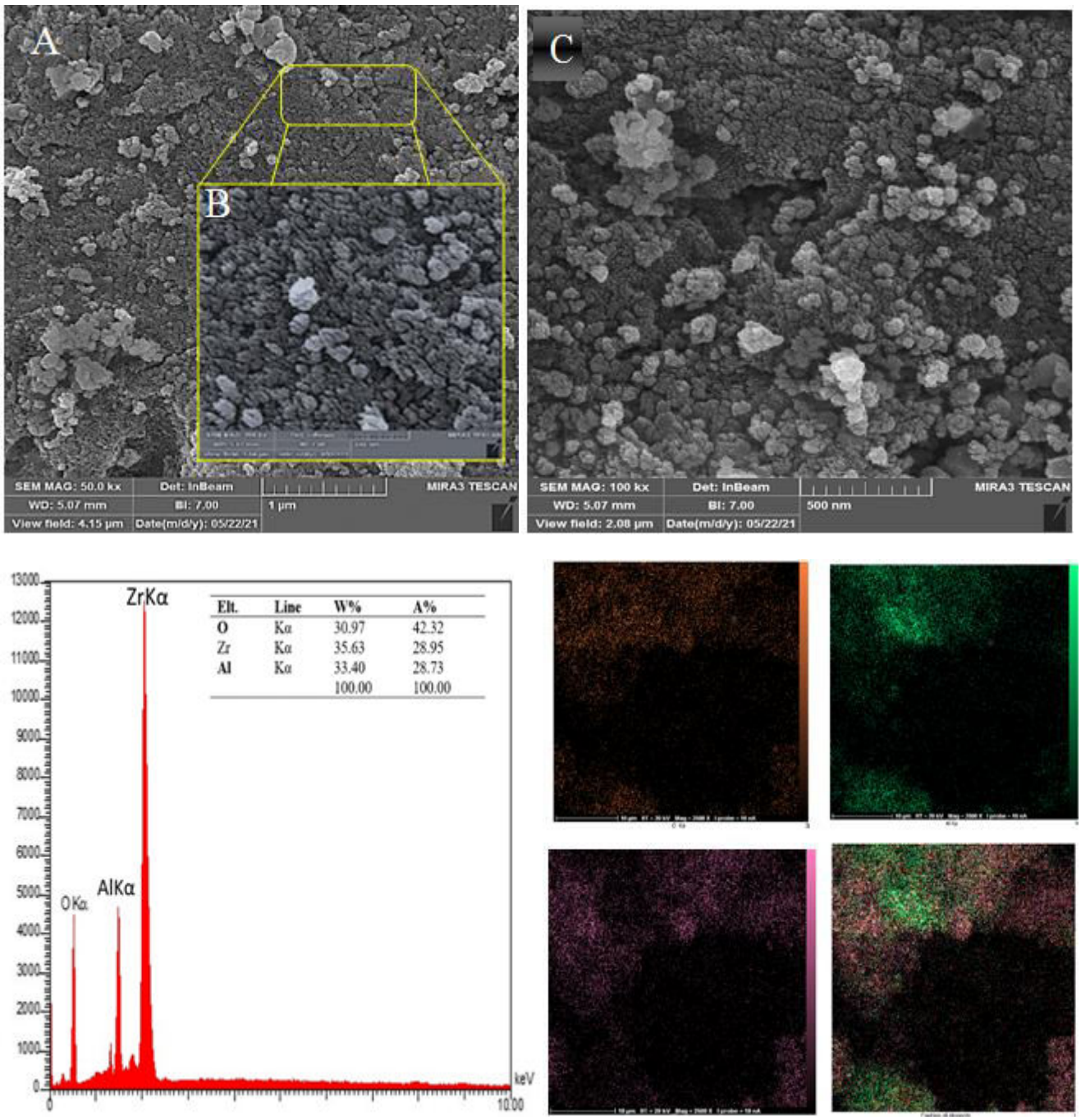

Figure-2. FESEM images describe the surface morphology of the (ZrO_2:Al_2O_3) specimen with different magnifications (A) 50KX, (B) 200KX and (C) 100 KX and elemental mapping of ZrO_2:Al_2O_3.

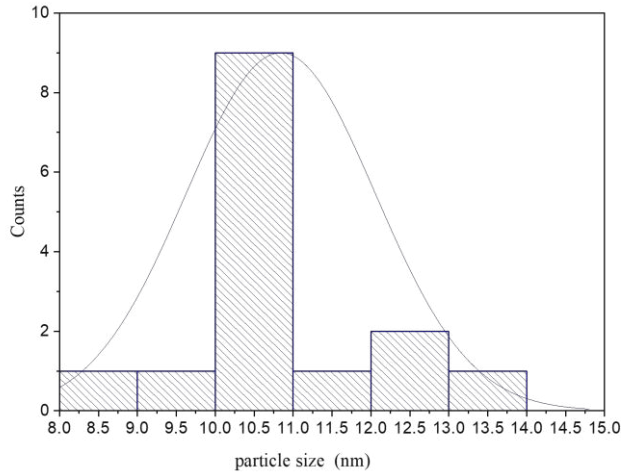

Figure-3. Particle size distribution histogram of ZrO_2:Al_2O_3. determined from the FESEM images.

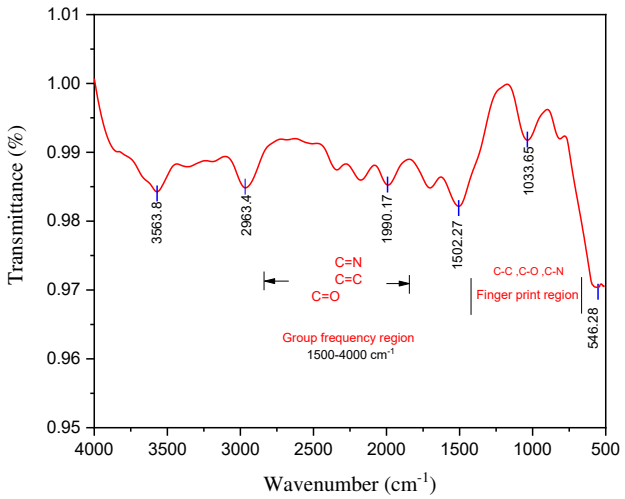

Figure-4. The FTIR spectrum of ZrO_2:Al_2O_3CNc.

ACKNOWLEDGEMENTS

With the support of the graduate laboratory of the physics department in the College of Science, Wasit University, Iraq, the experimental phase of the ZrO_2:Al_2O_3CNc production using the sol-gel technique. XRD, FESEM, E.D.X., and FTIR measurements of ZrO_2:Al_2O_3CNc were carried out at the central laboratory of the University of Tehran in Tehran, Iran.

REFERENCES

[1] A. D. Silva, E. M. Pallone and A. O. J. J. o. t. A. C. S. Lobo. 2020. Modification of surfaces of alumina-zirconia porous ceramics with Sr 2+ after SBF. 56(2): 517-524.

[2] O. Roualdes, M.-E. Duclos, D. Gutknecht, L. Frappart, J. Chevalier and D. J. J. B. Hartmann. 2010. In vitro and in vivo evaluation of an alumina–zirconia composite for arthroplasty applications. 31(8): 2043-2054.

[3] A. De Aza, J. Chevalier, G. Fantozzi, M. Schehl and R. J. B. Torrecillas. 2002. Crack growth resistance of alumina, zirconia and zirconia toughened alumina ceramics for joint prostheses. 23(3): 937-945.

[4] R. Benzaid *et al.* 2008. Fracture toughness, strength and slow crack growth in a ceria stabilized zirconia-alumina nanocomposite for medical applications. 29(27): 3636-3641.

[5] C. Hadjicharalambous, A. Buyakov, S. Buyakova, S. Kulkov and M. J. B. M. Chatzinikolaidou. 2015. Porous alumina, zirconia and alumina/zirconia for bone repair: fabrication, mechanical and in vitro biological response. 10(2): 025012.

[6] K. S. Masters and K. S. J. A. i. C. E. Anseth. 2004. Cell–material interactions. 29: 7-46.

[7] Y. Kimura, K. Matsuzaka, M. Yoshinari and T. J. D. m. j. Inoue. 2012. Initial attachment of human oral keratinocytes cultured on zirconia or titanium. pp. 2011-189.

[8] K. J. B. Anselme. 2000. Osteoblast adhesion on biomaterials. 21(7): 667-681.

[9] K. A. J. I. j. o. a. c. t. Hing. 2005. Bioceramic bone graft substitutes: influence of porosity and chemistry. 2(3): 184-199.

[10] K.-S. Lew, R. Othman, K. Ishikawa and F.-Y. J. J. o. B. A. Yeoh. 2012. Macroporous bioceramics: a remarkable material for bone regeneration. 27(3): 345-358.

[11] S. Thakur, S. Massou, A. Benoliel, P. Bongrand, M. Hanbucken and K. J. N. Sengupta. 2012. Depth matters: cells grown on nano-porous anodic alumina respond to pore depth. 23(25): 255101.

[12] V. Karageorgiou and D. J. B. Kaplan. 2005. Porosity of 3D biomaterial scaffolds and osteogenesis. 26(27): 5474-5491.

[13] D. Sarkar, D. Mohapatra, S. Ray, S. Bhattacharyya, S. Adak and N. J. C. i. Mitra. 2007. Synthesis and characterization of sol-gel derived ZrO2 doped Al2O3 nanopowder. 33(7): 1275-1282.

[14] A. A. Thamir, N. J. Jubier and J. F. Odah. 2021. Antimicrobial Activity of Zirconium Oxide

Nanoparticles Prepared by the Sol-Gel Method. In Journal of Physics: Conference Series. 2114(1): 012058: IOP Publishing.

[15] O. Mangla and S. Roy. 2018. Monoclinic zirconium oxide nanostructures having tunable band gap synthesized under extremely non-equilibrium plasma conditions. in Multidisciplinary Digital Publishing Institute Proceedings. 3(1): 10.

[16] Y. Hao, J. Li, X. Yang, X. Wang, L. J. M. S. Lu and E. A. 2004. Preparation of ZrO2–Al2O3 composite membranes by sol-gel process and their characterization. 367(1-2): 243-247.

[17] H. Nayebzadeh, N. Saghatoleslami and M. J. J. o. N. i. C. Tabasizadeh. 2019. Application of microwave irradiation for fabrication of sulfated ZrO 2-Al 2 O 3 nanocomposite via combustion method for esterification reaction: process condition evaluation. 9(2): 141-152.

[18] H. Lim, A. Ahmad and H. Hamzah. 2013. Synthesis of zirconium oxide nanoparticle by sol-gel technique. In AIP Conference Proceedings, 1571(1): 812-816: American Institute of Physics.

[19] D. Fang *et al*. 2013. Photoluminescence properties and photocatalytic activities of zirconia nanotube arrays fabricated by anodization. 35(7): 1461-1466.